Bulletin of Geosciences, Vol. 79, No. 4, 221–229, 2004

Late Variscan Sušice dyke swarm (Moldanubian Zone): quartz micromonzodiorite dykes and their pyroxene gabbro xenoliths

Stanislav Vrána

Czech Geological Survey, Klárov 3, CZ-118 21 Praha, E-mail: vrana@cgu.cz

Abstract. The N-S trending dyke swarm located east of Sušice in south-western Bohemia is of augite quartz micromonzodiorite composition. These fine-grained, equigranular, non-porphyritic rocks include rare amygdaloidal varieties. They are of subalkaline/tholeiitic, metaluminous (A/CNK = 0.8–0.9) composition, with a relatively low *mg* # and low Cr and Ni contents. Sr–Nd isotope analyses of three samples yielded initial $^{87}Sr/^{86}Sr = 0.708$ and $T_{Nd}^{DM} \approx 1.2–1.4$ Ga. The dykes carry rare xenoliths of two-augite gabbro (with Fe-rich A1 augite and Mg-rich A2 augite, $^{87}Sr/^{86}Sr$ also ~ 0.708) and dispersed small xenocrysts of A1 augite. The early Fe-rich A1 augite indirectly indicates derivation of the xenoliths from a fractionated gabbro intrusion below the present erosion level. Rare xenoliths of biotite paragneiss exhibit selective melting of feldspars and the devitrification of glass into fibrous and skeletal feldspar aggregates. The Sušice dykes are most likely of Permian age, as suggested by previous paleomagnetic study, as well as by the dating of primary hornblende (272 Ma) in dykes from Ševětín that resemble those from Sušice in terms of petrology, whole-rock chemistry, and Sr–Nd isotopic composition. The dyke swarm is spatially related to the circular Sušice structure expressed in the surface topography, but there is insufficient evidence for determining a causal link.

Key words: pyroxene quartz micromonzodiorite, dyke swarm, gabbro xenoliths, southern Bohemia, Moldanubian Zone

Introduction

Several dykes of augite quartz micromonzodiorite have been found in the Moldanubian Zone of south-western Bohemia between Sušice and Strakonice (referred to here as the Sušice dyke swarm). These non-porphyritic, partly amygdaloidal, fine-grained rocks, which could be alternatively classed as trachyandesite, are products of high-temperature magmatic crystallization at a relatively shallow intrusion level. Due to the multitude of dyke types in this part of the Moldanubian Zone (Holub et al. 1993), generally interpreted as being associated with the Variscan granitoid intrusions of the Central Bohemian Pluton (Žežulková 1982, 1989) and the Moldanubian Pluton, this distinct group of Sušice dykes has been largely overlooked so far.

The Sušice dykes arosed attention due to their similarity to augite microgranodiorite dykes near Ševětín, NNE of České Budějovice (Vrána et al. 1993, Košler et al. 2001). Paleomagnetic studies at one locality of the Sušice dykes indicated a probable Early Permian crystallization age (Krs and Vrána 1993). Similarly, Ar-Ar dating of titanian pargasite in one Ševetín dyke yielded an Early Permian (Upper Autunian) age (272 ± 2 Ma: Košler et al. 2001). In view of the geological evidence that the Sušice dykes represent the youngest igneous rocks in the area, and their paleomagnetic and petrological similarity to the Ševětín dykes, the Sušice dyke swarm is probably related to Permian volcanic activity in the Moldanubian Zone. While Permian volcanism produced large volumes of basaltic, andesitic, and rhyolitic rocks in the Saxothuringian Zone of northern Bohemia and Saxony (Prouza 1994), evidence of this activity in the Moldanubian Zone of the Bohemian Massif has been recognized only recently (Košler et al. 2001). Current geophysical models of the Moldanubian crust (Tomek et al. 1997) do not consider the possible role of Permian igneous activity, which could have potentially affected the structure and composition of the middle and lower crust of this tectonic zone.

Geological setting

The studied area is part of the Moldanubian Zone of SW Bohemia. It is comprised mainly of sillimanite-biotite paragneiss and migmatite, leucocratic biotite migmatite, and orthogneiss. Calcite marble and calc-silicate gneiss intercalations are widespread in the paragneiss-migmatite units north of Strakonice and northeast of Sušice (Fig. 1). In the north, the metasedimentary complex was intruded by granitoids of the Central Bohemian Pluton. The hornblende-biotite Červená granodiorite forms an arcuate body near Sušice, gently dipping to the northwest. Granitoids of the Moldanubian Pluton occur in the southwest, along the border with Germany (Fig. 1). Much of the area shows the NE-SW structural trend typical of the Bohemian branch of the Moldanubian Zone, though this domain adjoins the NW-SE trending Šumava (Bohemian Forest) structural domain 7 km SW of Sušice.

Analytical techniques

Whole-rock chemical analyses were performed in the laboratories of the Czech Geological Survey in Prague. Minor and trace element abundances were determined by XRF (Cr, Ni, Zn, Rb, Sr, Y, Nb, Sn, Ba and U) and INAA by the company Geoindustria, in Černošice, Czech Republic.

Table 1. Localities of analysed augite quartz micromonzodiorite samples

Sample No.	Locality
SN 15 and SN 16	Žichovice, 1.3 km south of the village and 100 m east of the road, loose blocks
SN 18	Kadešice, blocks 100 m SW of the village
SN 24	Kadešice, blocks 200 m SW of the village
SN 28	Nezdice, outcrop at the eastern edge of elevation above the quarry; 0.5 km north from the centre of Nezdice

Mineral composition was analysed by an electron microprobe Cam-Scan 4-90DV, equipped with EDX at the Czech Geological Survey. An accelerating voltage of 15 kV, a beam current of 3 nA, a counting time of 80 s, and ZAF correction program were used. Natural minerals were used as standards.

Three micromonzodiorite samples and one gabbro xenolith were analysed for Rb–Sr isotopic composition in the laboratories of the Czech Geological Survey. Three Sm-Nd isotopic analyses were performed in the Laboratory of the Mineralogical–Geological Museum in Oslo, Norway. The analytical methods were described in Vrána et al. (1993).

Note on augite terminology

The studied rocks contain three generations of augite of distinct compositions. The simple nomenclature of pyroxenes (Morimoto et al. 1988) does not provide a detailed designation for these individual generations. To assist our description, the augite types are designated as follows: A1 augite (Wo 26.7–40.0 mol.%, Fs 26.8–34.7); A2 augite (Wo 40.9–43.1, Fs 11.2–12.3); A3 augite (Wo 35.0–46.8, Fs 18.5–30.6). A1 and A2 augites occur in the rare gabbro xenoliths and as xenocrysts in the quartz micromonzodiorite. A3 augite is a major mineral in the quartz micromonzodiorite dykes.

Field relations and petrography

The micromonzodiorite dykes considered here are several metres wide. About 10% of the material shows amygdaloidal texture, with amygdales 2 to 7 mm in diameter, filled by calcite, minor quartz or chlorite, and rare K-feldspar (Fig. 2). Xenoliths of the paragneiss country rock and vein quartz occur in minor quantities. Rare xenoliths of two-pyroxene gabbro were sampled at a locality 1.3 km south of Žichovice. The location of the analysed samples is shown in Table 1.

In the augite quartz micromonzodiorite, crystallization started with minute tabular ilmenite, calcic plagioclase (An 65–45), and A3 augite, with lath-shaped plagioclase and anhedral A3 augite intergrown in a subophitic structure (Fig. 3). The anorthite content in zoned plagioclase declines outward, to values as low as An 10 (Fig. 4a). Wedge-shaped spaces among plagioclase crystals are partly filled by micrographic K-feldspar-quartz intergrowths. The feldspar and pyroxene compositions of one of the dykes are shown in Fig. 4, and representative mineral analyses are presented in Table 2. Opaque minerals have been identified by reflected light microscopy, microprobe analyses, and for a single dyke by thermal demagnetization of a whole-rock sample (Krs and Vrána 1993). Ilmenite and pyrrhotite are the main opaque phases, while pyrite, chalcopyrite, sphalerite, and galena occur only in trace amounts. Magnetite is absent. Minor chlorite, calcite, actinolite, muscovite, prehnite, and titanite probably crystallized during a late autohydrothermal stage.

Several generations of calcite, including massive calcite veins and drusy calcite coatings in open fractures, are associated with a thick calcite marble intercalation near Nezdice, close to one of the Sušice dykes (Žák et al. 1997). It is probable that some of the late

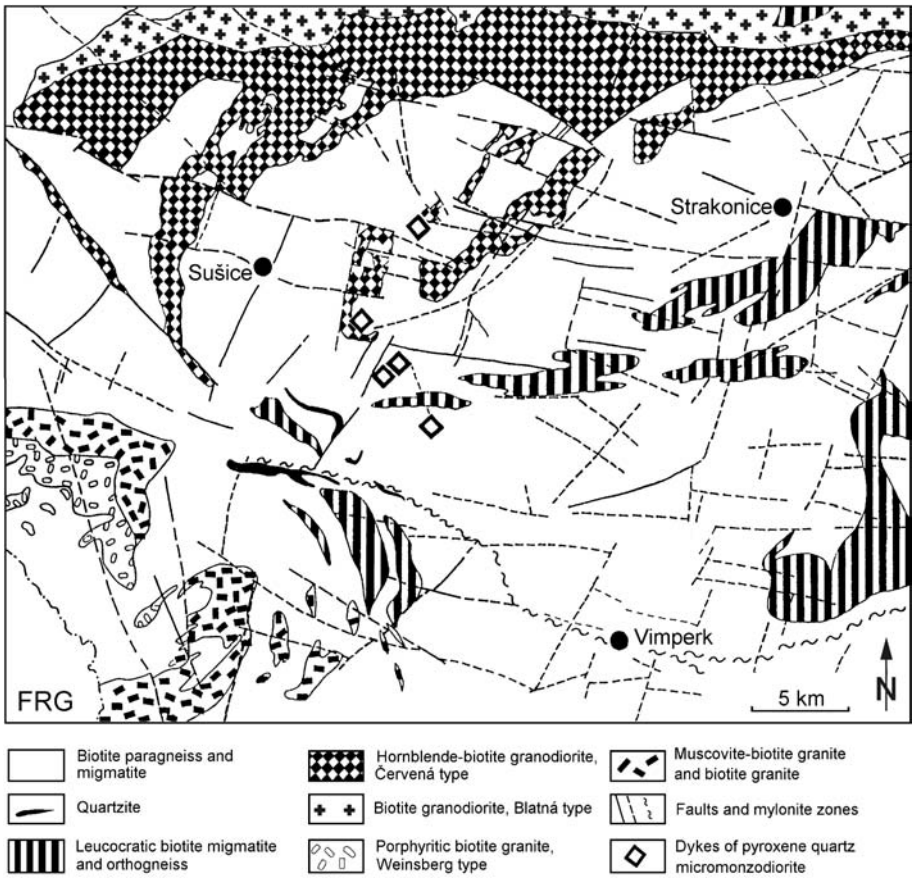

Figure 1. Geological sketch of the area around Sušice. Based on 1 : 50,000 maps published by the Czech Geological Survey.

calcite generations correlated with the thermal/fluid conditions during the intrusion of the Sušice dykes.

Chemical and isotopic composition

The chemical composition of the augite quartz micromonzodiorite dykes is presented in Table 3. As demonstrated by the multicationic plot of Debon and Le Fort (1983), these dykes are exclusively quartz monzonitic in composition (Fig. 5). In the diagram of Le Bas et al. (1986), five samples fall into the subalkaline/tholeiitic field. Three samples plot very near the quadruple point of basaltic trachyandesite-trachyandesite-basaltic andesite-andesite fields, while two samples plot close to the alkali-rich part of the andesite field. The rocks are metaluminous with A/CNK = 0.8–0.9, and have relatively low *mg* # and low Cr and Ni contents, indicating a prevalence of crustal material over primary mantle-derived melt.

The Sr-Nd isotopic composition of three samples with initial Sr values near 0.708 and $\varepsilon^{i}_{Nd} = -2.8$ to –5.1 (Table 4) indicates an important crustal component. The spread in ε^{i}_{Nd} values probably points to variation in the proportion of primary mantle melt and assimilated crustal material.

Gabbro xenoliths

Rare small clasts of two-augite gabbro, up to 4 cm long, have been found in one of the Sušice dykes 1.3 km SE of Žichovice. The mineral composition of the gabbro xenoliths is given in Table 5. Planimetric analysis of one xenolith (Fig. 6a) gave the following results (2400 points, vol.%): 30.7 A1 augite, 13.2 A2 augite, 55.0 plagioclase An 68–77, 1.1 ilmenite. The rock also contains traces of K-feldspar and sodic oligoclase.

The Fe-rich A1 augite (Wo 27 to 40) is unusual in having a Mg/Fe ratio near unity, and thus plotting in the pyroxene miscibility gap, indicating high cooling rates and crystallization in a dry system. Textural information shows that the crystallization of A1 augite was followed by that of a Mg-rich A2 augite, the latter of which forms relatively large oikocrysts (Fig. 6b). A1 augite is associated with bytownite (An 73). This is in contrast to layered intrusions, where the crystallization of Fe-rich augite usually occurs relatively late, i.e. in the ferrodiorite stage, and is accompanied by oligoclase-andesine (An<50). The gabbro xenoliths are completely free of primary (OH)-bearing minerals.

In addition to small gabbro xenoliths, relatively abundant A1 augite xenocrysts up to 3 mm long are scattered throughout the micromonzodiorite matrix. These xenocrysts have been observed in numerous sawn slices of the rock about 20 by 20 cm in size. They indicate (1) the tendency of entrained gabbro xenoliths to completely disaggregate, and (2) the original entrainment of augite gabbro was somewhat larger than indicated by the rare and small gabbro xenoliths.

The original A1 augite in the gabbro xenoliths and xenocrysts has unmixed into alternating lamellae of low-Ca pyroxene and high-Ca pyroxene (augite) as thin as 1–3 μm. This lamellar texture, observed in BSE images, indicates an approximate volume ratio of the two sets near unity. According to Deer et al. (1997), the unmixing of

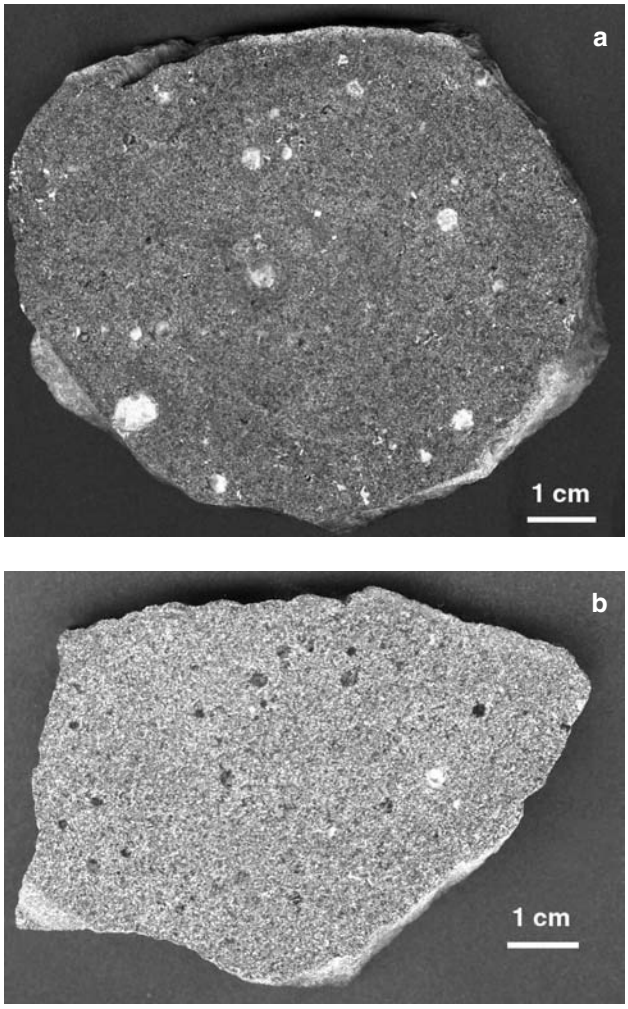

Figure 2. a – Amygdaloidal texture of augite quartz micromonzodiorite from the Žichovice locality. White amygdales are composed mainly of calcite. b – Amygdaloidal texture of augite quartz micromonzodiorite from Kadešice. Dark amygdales are coloured by chlorite.

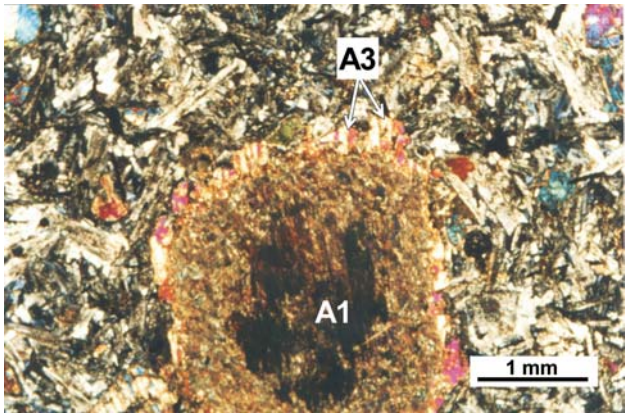

Figure 3. Photomicrograph of augite quartz micromonzodiorite from Žichovice. A1 augite xenocrysts (A1) are largely altered into smectite-like minerals and overgrown by A3 augite crystallized from micromonzodiorite magma. Crossed polarizers.

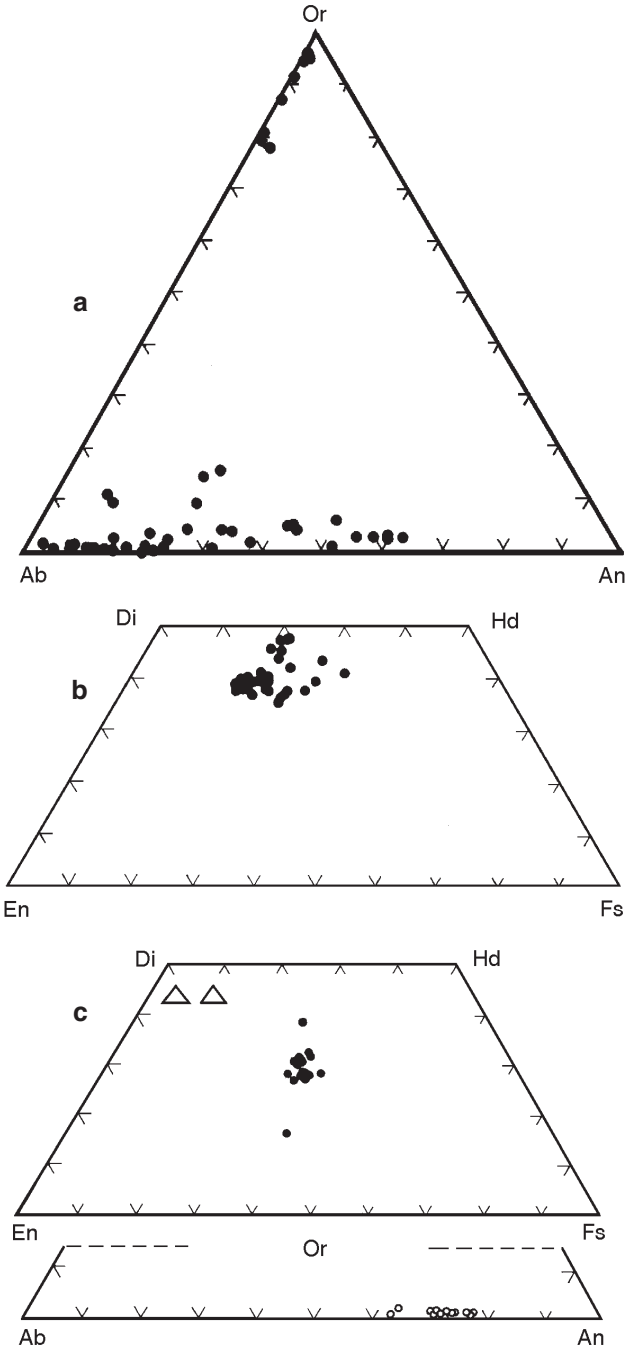

Figure 4. a – Feldspar and, b – A3 augite composition in the quartz micromonzodiorite dyke; c – composition of A1 augite (solid circles), A2 augite (triangle), and calcic plagioclase in a gabbro xenolith from a quartz micromonzodiorite dyke, locality south of Žichovice.

pyroxene solid-solutions with compositions in the centre of the pyroxene quadrilateral results in a lamellar structure comprised of augite and a low-Ca pyroxene, either pigeonite or orthopyroxene. In the present case, the average composition of A1 augite indicates the probable presence of unmixed pigeonite as the low-Ca component. All A1 augite analyses (Table 5, Fig. 4c) represent mixtures of the two sets of lamellae, as the electron beam diameter used in microprobe analysis is near 3 μm, while the lamellae are 1–3 μm wide. Calculation of the crystal chemical formulas for A1 augite (Table 5) indicates a slight surplus of silica, an absence of Al in tetrahedral sites, an absence of calcu-

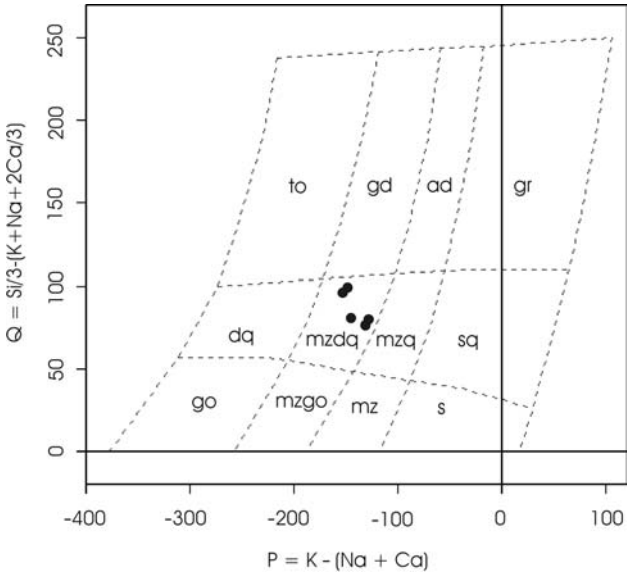

Figure 5. Composition of Sušice dyke rocks in the Debon and Le Fort (1983) diagram. Explanation: to – tonalite, gd – granodiorite, ad – adamellite, gr – granite, dq – quartz diorite, mzdq – quartz monzodiorite, mzq – quartz monzonite, sq – quartz syenite, go – gabbro, mzgo – monzogabbro, mz –monzonite, s – syenite.

lated Fe^{3+}, and a very small potassium content. This possibly indicates incipient alteration on a sub-microscopic scale within the A1 augite.

The A1 augite xenocrysts are largely altered into smectite-like pseudomorphs with some relict pyroxene. They typically carry overgrowths of A3 augite, chemically similar to the augite in the micromonzodiorite host-rock (Fig. 3).

Quartz and paragneiss xenoliths

One xenolith of biotite paragneiss rich in quartz, eight cm long, was sampled from the blocks of an amygdaloidal micromonzodiorite dyke at Kadešice. The xenolith bears evidence of the selective melting of feldspars and the later devitrification of feldspar glass into skeletal, radiating, and sheaf-like fibrous feldspar aggregates (Fig. 7). This probably indicates temperatures near 1100–1200 °C. The associated quartz was not melted, though it shows fracturing, fuzzy extinction grid patterns, nearly parallel cleavages, and local annealing recrystallization.

Several minor aggregates of fibrolitic sillimanite were observed in some micromonzodiorite thin sections as isolated heterogeneous inclusions. They apparently represent the refractory residua of nearly digested sillimanite-biotite paragneiss xenoliths.

The Sušice structure

The Sušice dyke swarm coincides with the Sušice circular structure expressed in the surface topography. This structure is exposed on the NE erosional slope of the Bohemian Forest (Šumava Mts.). The surface morphology of the Sušice structure (Fig. 8), derived as a computer model from 1 : 50,000

Table 2. Composition of minerals in quartz micromonzodiorite, sample SN 18

Mineral	A3 Augite				Plagioclase			K-feldspar
Analysis No.	25	16	S3	S1	PS1	15	21	32
SiO_2	51.23	51.30	51.19	53.01	53.31	55.75	66.61	65.47
TiO_2	0.89	1.16	0.28	0.38	0.00	0.00	0.00	0.00
Al_2O_3	1.82	2.41	1.39	0.89	28.49	27.56	20.80	18.14
FeO^t	15.41	11.60	17.54	12.91	0.51	0.17	0.22	0.30
MnO	0.32	0.27	0.80	0.45	0.00	0.00	0.00	0.00
MgO	12.25	14.26	9.64	10.59	0.61	0.16	0.00	0.14
CaO	16.71	18.16	17.78	22.36	12.12	10.84	2.13	0.00
Na_2O	0.54	0.62	0.44	0.38	4.20	5.58	10.20	0.64
K_2O	0.00	0.00	0.00	0.00	1.14	0.24	0.10	15.64
Total	99.16	99.77	99.04	100.96	100.39	100.30	100.06	100.32
Cations	4	4	4	4	20	20	20	20
Si	1.963	1.920	1.995	2.000	9.622	10.013	11.738	12.068
Ti	0.025	0.032	0.008	0.010	–	–	–	–
Al	0.081	0.106	0.063	0.039	6.061	5.834	4.320	3.941
Fe^{3+}	–	0.032	–	–	0.427	0.137	–	–
Fe^{2+}	0.494	0.330	0.572	0.407	–	–	0.032	0.046
Mn	0.010	0.009	0.026	0.014	–	–	–	–
Mg	0.700	0.796	0.560	0.596	0.164	0.042	–	0.038
Ca	0.686	0.728	0.742	0.904	2.344	2.086	0.402	–
Na	0.040	0.044	0.033	0.027	1.470	1.943	3.485	0.229
K	–	–	–	–	0.263	0.054	0.022	3.678
Wo	31.59	32.00	34.93	44.02				
En	34.39	38.63	28.05	29.72				
Fs	24.27	16.04	28.63	20.33				
An					57.50	51.08	10.29	0.00
Ab					36.06	47.58	89.14	5.86
Or					6.44	1.35	0.58	94.14

altitude contour maps with 100 m altitude interval, features a moderately distinct circular symmetry owing to delicate erosional etching and strong relief (ca 400–1300 m a.s.l.). The second circle from the centre in Fig. 8, ~ 18 km in diameter, coincides in its western part with the arcuate course of the Otava River. The structure is not convincingly identified in gravimetry and airborne magnetometry maps, but has been inferred from satellite photographs (Dornič and Šťovíčková 1984) and preliminary airborne magnetometry data (Šalanský 1987). The geologic map shows a prominent semi-annular, shallow-dipping body of hornblende-biotite granodiorite (Červená type) in the north-western sector, and smaller steeply-dipping bodies of leucocratic migmatite and orthogneiss (Fig. 1).

Discussion and conclusions

The significance of the two-augite gabbro xenoliths and A1 augite xenocrysts

The two-augite gabbro xenoliths and A1 augite xenocrysts identified in the micromonzodiorite are indicative of the complicated history of the A1 augite. An Fe-rich A1 augite cumulate, presumably a product of the fractional crystallization of a ferrodioritic melt in a hypothetical magma chamber, became disintegrated and engulfed by a later batch of gabbroic magma. The crystallization of this melt with dispersed A1 augite xenocrysts resulted in the formation of a two-augite gabbro (Figs 6 and 7). Such a scenario explains the compositional differences of the pyroxenes in the two-augite gabbro xenoliths in contrast to the typical evolution of layered gabbro intrusions, e.g. Skaergaard and Bushveld (Fig. 9). The broken arrow for Sušice xenoliths in Fig. 9, from A1 augite to Mg-rich A2 augite, running in an opposite direction to those of layered gabbro intrusions, indicates a time sequence of crystallization rather than continuous evolution in a coherent magma batch. These relations point to three successive stages of coexistence of the A1 augites with various melts: (i) A1 augite precipitated from a ferrodiorite melt; (ii) an A1 augite accumulation was engulfed by a later batch of gabbroic magma; (iii) disaggregation of two-augite gabbro xenoliths in the micromonzodiorite melt that generated the Sušice dykes.

The petrological information extracted from xenoliths and xenocrysts in the Sušice dykes indicates the probable

Table 3. Chemical composition of pyroxene quartz micromonzodiorite dykes

Location	Žichovice		Kadešice		Nezdice
Sample No.	SN 15	SN 16	SN 18	SN 24	SN 28
SiO_2	54.74	55.09	56.44	55.95	58.08
TiO_2	1.55	1.59	1.27	1.28	1.25
Al_2O_3	15.55	15.66	16.57	16.49	16.55
Fe_2O_3	1.81	1.81	1.22	1.37	1.44
FeO	6.29	6.37	4.99	4.99	5.21
MnO	0.134	0.135	0.102	0.101	0.10
MgO	4.13	4.06	3.99	3.89	4.29
CaO	6.20	6.11	6.66	5.93	6.44
Li_2O	0.008	0.008	0.004	0.005	0.008
Na_2O	2.58	2.76	2.54	3.07	2.88
K_2O	3.14	3.18	2.52	2.83	2.63
P_2O_5	0.25	0.25	0.25	0.26	0.27
CO_2	0.33	0.04	0.20	0.44	0.34
C	0.06	0.05	0.05	0.08	0.03
H_2O^+	2.52	2.64	2.33	2.69	2.36
F	0.073	0.059	0.063	0.073	0.08
S	< 0.01	< 0.01	< 0.01	< 0.01	0.05
H_2O^-	0.17	0.12	0.08	0.10	n.d.
Total	99.50	99.91	99.25	99.52	101.94
Minor and trace elements (ppm)					
Be	3	3	3	3	2
B	15	15	< 9	< 9	< 9
Sc	31	29	23	23	n.d.
V	128	124	86	86	89
Cr	41	43	74	73	75
Co	29	28	17	18	18
Ni	10	10	11	11	12
Cu	10	8	11	8	13
Zn	69	68	65	69	84
As	17	14	12	38	n.d.
Rb	148	132	78	108	84
Sr	415	377	324	355	373
Y	26	27	23	24	26
Zr	207	204	243	244	244
Nb	7	6	10	13	15
Mo	1	1	2	1	2
Sn	3	3	4	5	6
Cs	3.9	2.7	0.8	0.9	n.d.
Ba	705	749	756	826	738
La	40	40	45	46	n.d.
Ce	71	69	84	84	n.d.
Nd	42	41	48	47	n.d.
Sm	7.9	8.3	8.9	9.0	n.d.
Eu	1.56	1.69	1.48	1.41	n.d.
Tb	1.2	1.3	1.1	1.3	n.d.
Yb	3.4	3.3	2.7	2.8	n.d.
Lu	0.40	0.55	0.38	0.37	n.d.
Hf	5	5	6	5.8	n.d.
Th	7.9	8.4	12.8	13.1	n.d.
U	2.8	2.0	2.2	3.1	n.d.

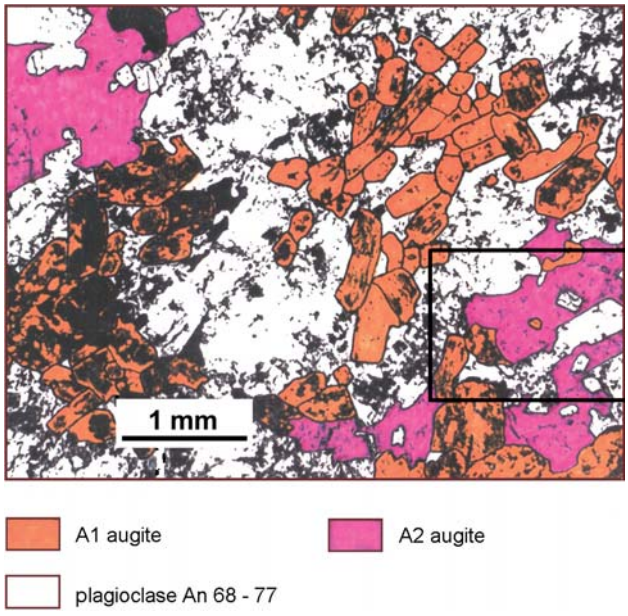

Figure 6a. Texture of the two-augite gabbro xenolith enclosed in an augite quartz micromonzodiorite dyke (Žichovice). The figure is a photocopy of a thin section, coloured to bring out the texture of the rock. The framed area is shown in Fig. 6b.

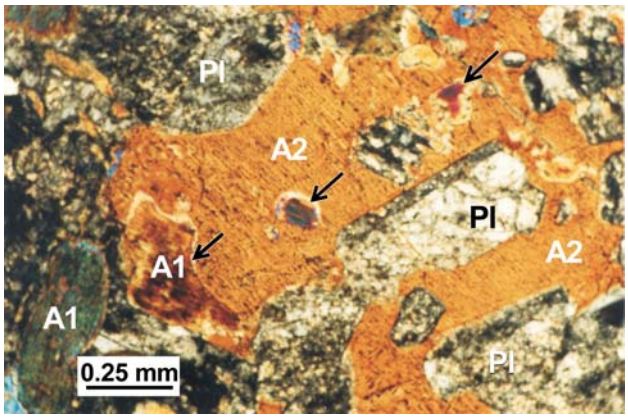

Figure 6b. Photomicrograph of a two-augite gabbro xenolith from an augite quartz micromonzodiorite dyke (Žichovice). A poikilitic crystal of A2 augite (A2) encloses euhedral plagioclase and A1 augite crystals (A1). Additional small inclusions of A1 augite are indicated by arrows. Crossed polarizers. See Fig. 6a for the location of this subarea.

existence of a gabbroic intrusion beneath the present surface. The Kdyně gabbro/diorite massif, the closest known basic complex, is located 30 km north-west of the Sušice dyke swarm (in the southern part of the Bohemicum). It is a tectonically segmented layered intrusion (Vejnar 1986) of Cambrian age (Bues 2002). As the Moldanubian Zone of south-western Bohemia is comprised of a heterogeneous blend of units assembled only during the Variscan orogeny, it is unlikely that the inferred gabbroic intrusion in the Sušice area can be correlated with the Kdyně massif. Differences in mineralogical composition (compare Vejnar 1986) also make such correlation unlikely. In particular, pigeonite (or orthopyroxene) – high-Ca clinopyroxene solid solutions, comparable to A1 augite in Sušice dykes and indicating relatively high cooling rates, have not been observed in the Kdyně massif. The possibil-

Table 4. Sr-Nd isotopic data for augite quartz micromonzodiorite
(age = 270 Ma)

Sample	Rb (ppm)	Sr (ppm)	$^{87}Rb/^{86}Sr$	$^{87}Sr/^{86}Sr$	2 s.e.	$^{87}Sr/^{86}Sr_i$
SN 15	136	437	0.9019	0.71185	3	0.70839
SN 16	127	393	0.9357	0.71175	3	0.70816
SN 18	64	329	0.5649	0.71031	3	0.70814
SN15K*	94	473	0.5754	0.71083	1	0.70862

Sample	Sm (ppm)	Nd (ppm)	$^{147}Sm/^{144}Nd$	$^{143}Nd/^{144}Nd$	2 s.e.	$^{143}Nd/^{144}Nd_i$	εNd_i	$T_{Nd}CHUR$	T^{DM}_{Nd} 2stg
SN 15	6.64	34.76	0.11548	0.512349	19	0.512145	–2.8	0.54	1.22
SN 16	6.78	34.16	0.11999	0.512351	10	0.512139	–3.0	0.57	1.23
SN 18	7.40	38.99	0.11473	0.512232	9	0.512029	–5.1	0.76	1.40

* sample SN15K is augite gabbro xenolith in micromonzodiorite

Table 5. Composition of minerals in two-augite gabbro xenolith, sample SN 15X

Mineral	A1 augite	A2 augite	illmenite	plagioclase	K-feldspar	albite
n*	9	4	4	2	3	2
SiO_2	52.48	52.13	0.27	50.40	65.70	66.00
TiO_2	0.07	0.74	52.02	0.00	0.10	0.20
Al_2O_3	2.27	2.59	0.06	31.45	18.10	19.80
Cr_2O_3	0.25	0.28	0.30	0.00	0.04	0.00
FeO^t	18.12	7.05	44.81	0.00	0.25	0.20
MnO	0.23	0.16	2.23	0.00	0.04	0.00
MgO	11.22	16.04	0.12	0.00	0.00	0.00
CaO	14.71	20.53	0.00	15.00	0.00	1.30
Na_2O	0.29	0.52	0.00	2.85	0.31	10.80
K_2O	0.06	0.00	0.00	0.30	16.50	0.10
Total	99.70	100.04	99.81	100.00	101.04	98.40
Cations	4	4	4	20	20	20
Si	2.021	1.915	0.013	9.165	12.055	11.774
Ti	0.002	0.020	1.975	–	0.013	0.026
Al	0.103	0.111	0.004	6.740	3.914	4.163
Cr	0.008	0.008	0.011	–	–	–
Fe^{3+}	–	0.046	0.008	–	–	–
Fe^{2+}	0.584	0.170	1.884	–	0.038	0.030
Mn	0.008	0.005	0.095	–	0.006	–
Mg	0.644	0.878	0.009	–	–	–
Ca	0.607	0.808	–	3.020	–	0.249
Na	0.021	0.037	–	1.005	0.110	3.735
K	–	–	–	0.069	3.862	0.022
Wo	32.95	42.35				
En	34.97	46.04				
Fs	32.09	11.61				
An				73.76	0.00	6.20
Ab				24.54	2.78	93.23
Or				1.70	97.22	0.57

n* = number of averaged analyses

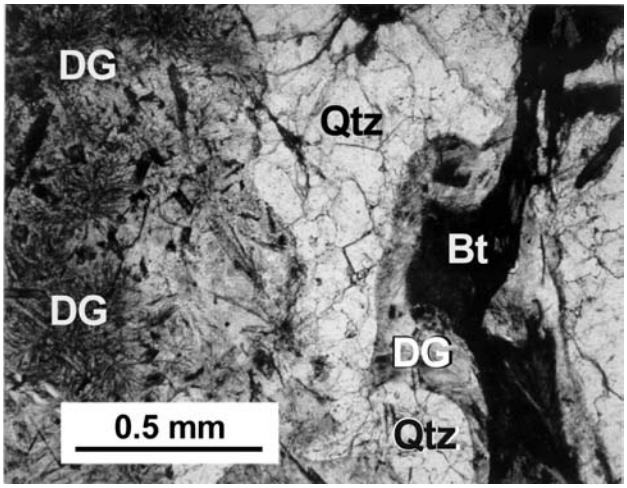

Figure 7. Partially molten biotite paragneiss xenolith from a quartz micromonzodiorite dyke (Kadešice). DG – devitrified glass composed of fibrous and skeletal feldspar aggregates; Qtz – quartz; Bt – biotite. Plane polarized light.

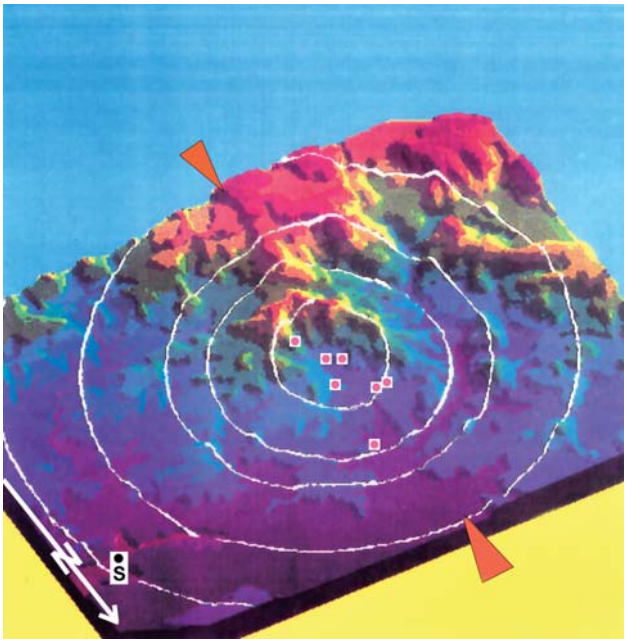

Figure 8. An axonometric view of the Sušice structure looking SW, computer-generated from level contour maps (100 m intervals). Illumination is from the NW. The model, 32 km wide, shows the erosional slopes of the Šumava Mts. (Bohemian Forest). Relief ranges from 400 m (bottom left) to 1 200 m a.s.l. (top right). The letter S in the lower left corner indicates the regional centre of Strakonice (cf. Fig. 1). The localities of quartz micromonzodiorite dykes are indicated by red circles. Orange arrows indicate a probable fault structure trending approximately N-S. Computer image by J. Flusar, Praha.

ity that the inferred intrusion is of Permian age thus remains open.

The relation of the Sušice dyke swarm to the Sušice circular structure

Owing to limited exposure, the present information on the quantity and distribution of the dykes is incomplete. The abundance of loose material from the dyke rocks 2 km SE

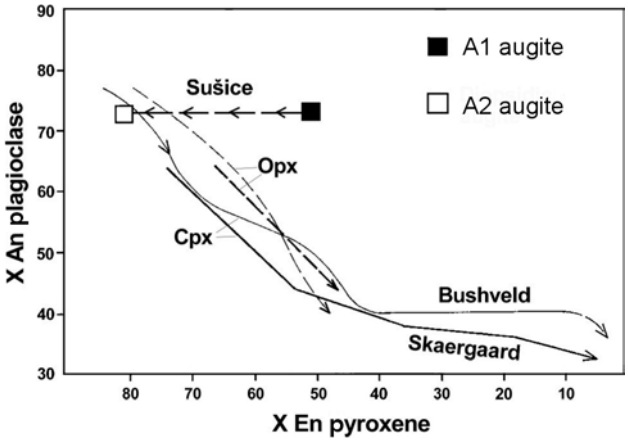

Figure 9. Plot of the mole fraction of anorthite in plagioclase versus the mole fraction of enstatite in pyroxene, showing two-augite gabbro xenolith from the micromonzodiorite Sušice dyke (locality Žichovice), compared to the Skaergaard and Bushveld fractionation trends (based on data by Wager and Brown 1968). Note that the dashed arrow for the Sušice two-augite gabbro xenolith indicates only the temporal (and not fractionation) sequence in the crystallization of the A1 and A2 augites. See text for discussion.

of Žichovice indicates the existence of a major dyke cluster in this region. Quaternary alluvial deposits in the Nezdice brook valley possibly cover additional dykes. With the existing information, it is not possible to prove a causal link between the intrusion of the dykes and the deformation of the upper crust responsible for the circular morphological form. Nonetheless, the dyke swarm runs through the centre of the structure (Fig. 8). One possible scenario would be a nearly circular cauldron-like subsidence triggered by the evacuation of a magma chamber. Such a cause is speculative at present, though the spatial coincidence is noteworthy indeed. Alternatively, the association of the dyke swarm with the circular structure could be only incidental.

The relation of the Sušice micromonzodiorite dykes to the augite microgranodiorite dykes near Ševětín

Although the Ševětín dykes are somewhat more felsic and richer in Cr and Ni than those of the Sušice swarm, there are several striking similarities. In both, the high-temperature mineralogy includes augite as the primary mineral. Both rock types are characterized by the absence of phenocrysts, a fine-grained structure, and the occasional presence of amygdales indicating a relatively shallow level of intrusion. The similarities in their $^{87}Sr/^{86}Sr$ ratios (0.708) and in their whole-rock Nd model ages calculated using the two-stage, depleted mantle model (T_{Nd}^{DM} ~ 1.2–1.4 Ga) (Liew and Hofmann 1988) are especially noteworthy. These model ages point to a significant depleted mantle component, in contrast to earlier Variscan granitoid rocks (Janoušek et al. 1995). Another related rock type seems to be the augite-biotite quartz monzodiorite of the Štěpánovice dyke near Lišov (Vrána and Janoušek 1999), which also gives a similar Nd model age of T_{Nd}^{DM} =1.2 Ga, even though its strontium is somewhat less radiogenic ($^{87}Sr/^{86}Sr$ ~ 0.7064). Elevated Cr and Ni indicate similarity to the Še-

větín microgranodiorite dykes. The Štěpánovice dyke and two additional related occurrences also show a high-temperature mineral assemblage, evinced by the rare presence of pyroxenes with compositions plotting in the central part of the pyroxene quadrilateral.

Acknowledgements. Jiří Bendl, formerly with the Czech Geological Survey, conducted Sr and Nd isotope analyses presented in Table 4. Vojtěch Janoušek calculated the isotopic ratios and model ages in Table 4 and provided helpful comments on early and late versions of the paper. Vladimír Žáček prepared several photomicrographs included in this paper. I am indebted to František Holub for a careful review of the manuscript.

References

Bues C. (2002): Emplacement depths and radiometric ages of Paleozoic plutons of the Neukirchen-Kdyně massif: differential uplift and exhumation of Cadomian basement due to Carboniferous orogenic collapse (Bohemian Massif). Tectonophysics 352, 225–243.

Debon F., Le Fort P. (1983): A chemical-mineralogical classification of common plutonic rocks and associations. Trans. R. Soc. Edinb. Earth Sci. 73, 135–149.

Deer W. A., Howie R. A., Zussman J. (1997): Rock-forming minerals, Vol. 2A, Single-chain silicates. The Geological Society, London.

Dornič J., Šťovíčková N. (1984): Linear and circular structures of the Bohemian Massif – comparison of satellite and geophysical data. Adv. Space Res. 4, 11, 115–121.

Holub F., Schulmann K., Táborská Š. (1993): Dyke swarms in the Central Bohemian Plutonic Complex. MS, Archive Czech Geological Survey, Praha. (in Czech)

Janoušek V., Rogers G., Bowes D. R. (1995): Sr-Nd isotopic constraints on the petrogenesis of the Central Bohemian Pluton, Czech Republic. Geol. Rdsch. 84, 520–534.

Košler J., Kelley S. P., Vrána S. (2001): $^{40}Ar/^{39}Ar$ hornblende dating of a microgranodiorite dyke: implications for early Permian extension in the Moldanubian Zone of the Bohemian Massif. Int. J. Earth Sci. 90, 379–385.

Krs M., Vrána S. (1993): Palaeomagnetism and petromagnetism of augite microgranodiorite, Nezdice near Kašperské Hory, southern Bohemia. J. Czech Geol. Soc. 38, 201–207.

Le Bas M. J., Le Maitre R. W., Streckeisen A., Zanettin B. (1986): A chemical classification of volcanic rocks based on the total alkali-silica diagram. J. Petrol. 27, 745–750.

Liew T. C., Hofmann A. W. (1988): Precambrian crustal components, plutonic associations, plate environment of the Hercynian Fold Belt of Central Europe: indications from a Nd and Sr isotopic study. Contr. Mineral. Petrology 98, 129–138.

Morimoto N. et al. (1988): Nomenclature of pyroxenes. Amer. Mineralogist. 73, 1123–1133.

Prouza V. (1994): Permo-Carboniferous limnic basins of the Bohemian Massif. In: Klomínský J. (ed.) Stratigraphy: Geological Atlas of the Czech Republic. Czech Geological Survey, Praha.

Šalanský K. (1987): Geofyzikální projevy cirkulárních struktur Českého masivu. MS Czech Geological Survey, Praha. (in Czech)

Tomek Č., Dvořáková V., Vrána S. (1997): Geological interpretation of the 9HR and 503M seismic profiles in western Bohemia. In: Vrána S., Štědrá V. (eds) Geological model of western Bohemia related to the KTB borehole in Germany. Sbor. geol. Věd, Geol. 47, 43–50.

Vejnar Z. (1986): The Kdyně massif, south-west Bohemia – a tectonically modified basic layered intrusion. Sbor. Geol. Věd, Geol. 41, 9–67.

Vrána S., Bendl J., Buzek F. (1993): Pyroxene microgranodiorite dykes from the Ševětín structure, Czech Republic: mineralogical, chemical and isotopic indication of a possible impact melt origin. J. Czech Geol. Soc. 38, 129–148.

Vrána S., Janoušek V. (1999): Petrologie a geochemie štěpánovické žíly pyroxen-biotitického křemenného monzodioritu. Zpr. geol. Výzk. v Roce 1998, 81–82. (in Czech)

Wager L. R., Brown G. M. (1968): Layered igneous rocks. Oliver and Boyd. Edinburgh.

Žák K., Dobeš P., Vrána S. (1997): Formation conditions of various calcite types and unusual alteration products of wollastonite in calcite marble near Nezdice (Varied Group of Moldanubicum), Czech Republic. J. Czech Geol. Soc. 42, 17–25.

Žežulková V. (1982): Dyke rocks in the southern part of the Central Bohemian Pluton. Sbor. geol. Věd, Geol. 37, 71–102. (in Czech)

Žežulková V. (1989): The sequence of dyke rocks of the Central Bohemian Pluton. Bull. Czech Geol. Surv. 64, 277–286. (in Czech)